Tasmania

Tasmanian Geological Survey
Record 2001/13

Glaucophane and phengite-bearing amphibolite, Port Sorell: Mineral composition and petrology

R. S. Bottrill

Abstract

Neoproterozoic amphibolites occurring near Port Sorell in northern Tasmania contain abundant blue, sodic to sodic-calcic amphiboles, mostly ferroglaucophane and ferrowinchite, plus phengitic muscovite, albite, actinolite, sphene and epidote. The assemblage and mineral chemistry suggest the original dolerite underwent partial greenschist facies metamorphism closely followed by blueschist facies metamorphism. There is some relict pyroxene (augite). The greenschist metamorphism was at about 300 MPa and 350–450°C, while minimum peak metamorphic conditions for phengite and blue amphibole were about 400–500°C and 1000–1410 MPa, which corresponds to a depth of burial of the order of 30 km in a low geothermal gradient.

Introduction

Blue, sodic to sodic-calcic amphiboles, suggesting possible high-pressure formation, were found by A. Reed (Reed et al., in prep.) in Neoproterozoic amphibolite near Port Sorell in northern Tasmania. The petrology and compositions of blue amphiboles and related minerals in the amphibolite are described in this report, and the conditions of metamorphism are interpreted.

Blue amphiboles (glaucophane and related sodic and sodic-calcic mineral phases) occur in lower Proterozoic to Cambrian rocks in various other areas of Tasmania, particularly in the Arthur Metamorphic Complex between Savage River and Reece Dam (Spry, 1964; Green and Spiller, 1977; Turner and Bottrill, 1993; Turner and Bottrill, 2001), and also near Wynyard (Everard, in prep.) and the Gordon River (Brown *et al.*, 1989). The Corinna amphibolite is interpreted to have formed under minimum conditions of 350°C and 700 MPa (Turner and Bottrill, 1993; 2001); the other occurrences appear to have formed under slightly lower pressure, but have not been fully evaluated.

Petrography

The amphibolite (Sample No. R007830, AMG 467 560 mE, 5 434 500 mN) is highly altered but still exhibits a strong remnant doleritic texture, with primary subophitic intergrowths of medium-grained plagioclase and pyroxene (both ~30%, <1 mm long; Plate 1). Skeletal opaque minerals (~5%; <0.5 mm) consist of mixtures of ilmenite, magnetite and sphene (?). There are large aggregates of yellow epidote and quartz to about 2 mm in size (~20%); these appear to represent altered phenocrysts in part, but some resemble amygdules. The groundmass (~20%) is a mixture of fine-grained muscovite (<30 µm diameter), quartz, albite, opaque minerals and blue amphiboles. Muscovite also occurs in sparse fine-grained clots to about 2 mm in size; these may represent altered K-feldspar phenocrysts (Plate 2). There is also some trace pyrite (<0.5 mm; mostly altered to limonite).

The brown clinopyroxenes are partly altered to coarse-grained, green, actinolitic amphibole (~5–10%; Plate 1). Blue amphiboles (~20%) mostly form rims and overgrowths (<1 mm) on this green actinolitic amphibole, but also occur as finer grains with quartz, epidote, albite and muscovite in the groundmass. No pumpellyite, garnet or chlorite were observed, and there is no indication of any late stage retrogression to greenschist facies. The rock shows little or no foliation.

Mineral compositions

Analytical procedures and formulae calculation

The amphiboles and associated minerals were analysed (Tables 1–4) with a Cameca SX-50 electron microprobe, using WDS spectrometers at 15 kV, at the University of Tasmania.

The amphibole formulae (Table 2) and calculated Fe^{3+} were determined from the analysed weight percent oxides using the methods of Schumacher (1997). The amphibole nomenclature is that of Leake *et al.* (1997).

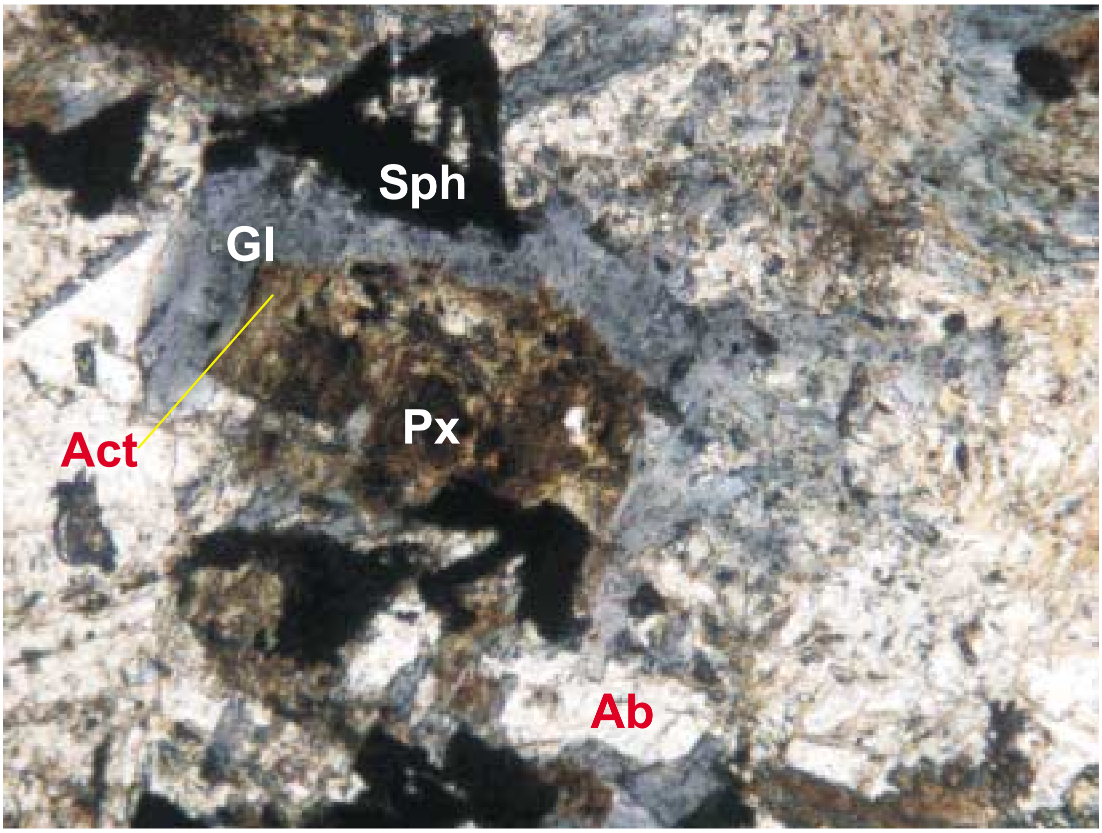

Plate 1. *Photomicrograph of brown augitic clinopyroxene partly replaced by greenish actinolite, replaced in turn by blue sodic amphibole, in a matrix of albitised plagioclase laths, altered magnetite/sphene, plus epidote (granular, yellow, high relief) and muscovite (colourless, low relief) in sample R007830A. Plane polarised light. Field of view: 1.1 × 0.7 mm.*
Gl = glaucophane; Act = actinolite; Px = pyroxene; Ab = albite; Sph = sphene.

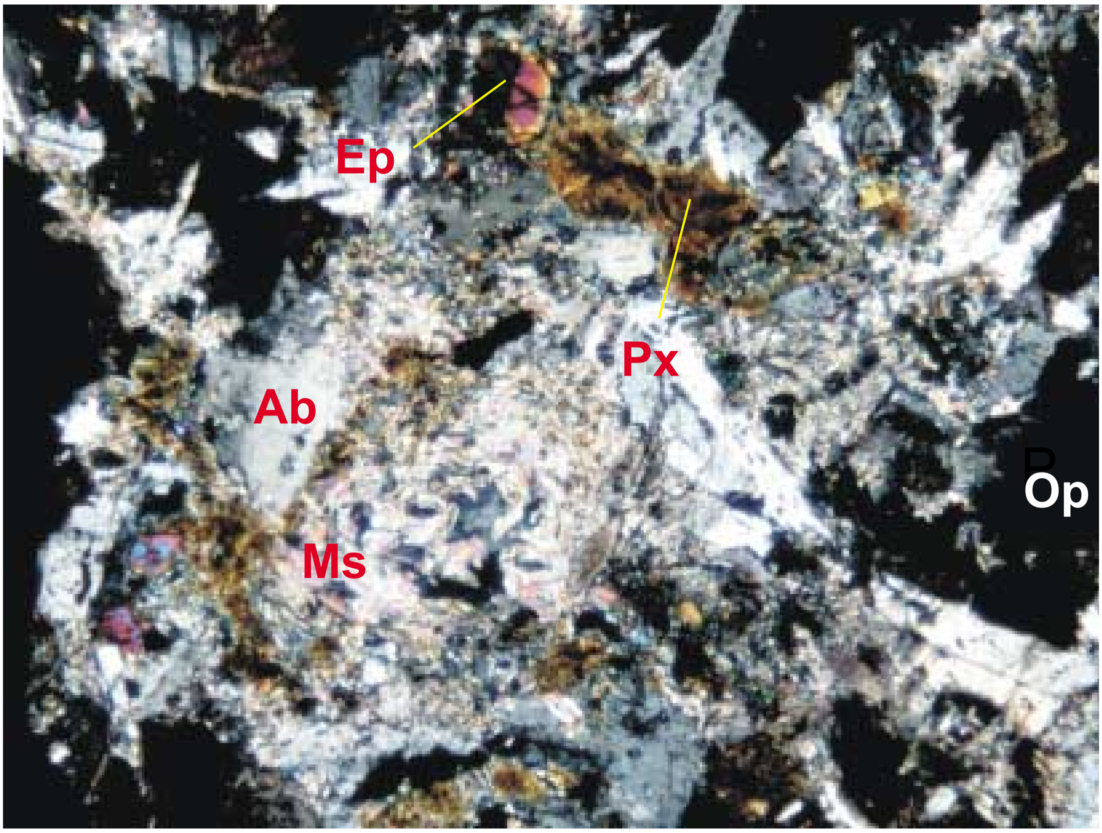

Plate 2. *Photomicrograph of a clot of phengitic muscovite (after K-feldspar?), with albitised plagioclase laths, brown, altered pyroxene, magnetite, plus epidote (granular, yellow, high relief)) in sample R007830B. Cross polarised light. Field of view: 1.1 × 0.7 mm.*
Ms = muscovite; Px = pyroxene; Ep = epidote; Ab = albite; Op = opaques.

To determine the mineral species the cation distributions were calculated in accord with the standard amphibole formula (op cit.): $AB_2C_5^{vi}T_8^{iv}O_{22}(OH,O,Cl,F)_2$. The FeO/Fe_2O_3 ratios were not determined separately but were calculated by crystal chemical considerations and the average of minimum and maximum constraints (Schumacher, 1997).

Pyroxene and epidote formulae and calculated Fe^{3+} were determined using the method of Schumacher (1991). The pyroxenes are aegirine-augites (Table 3). Mica formulae were determined assuming all Fe as FeO, as there are no simple crystallochemical constraints for constraining the FeO/Fe_2O_3 ratios. They are all phengitic muscovites (Table 1). The feldspars are albite (Table 4). A sphene was also analysed (Table 4).

Results and interpretation

The assemblage present supports a relatively high pressure–low temperature peak metamorphic facies. A petrogenetic grid for NCFMASH (Na_2O-FeO-MgO-(Al_2O_3+Fe_2O_3)-SiO_2-H_2O), based on pure systems for medium to high pressure metamorphic facies in basic assemblages, is shown in Figure 1. Glaucophane-ferroglaucophane indicates a relatively high pressure origin (>600 MPa). The lack of pumpellyite, lawsonite, hornblende and garnet in these rocks suggest the temperature of the high pressure metamorphic event to probably be constrained between about 400 and 500°C at 700–1200 MPa (fig. 5).

Analytical data for the blue amphiboles (Table 2) show that they range in composition from sodic-calcic (winchite, ferriwinchite, ferro-ferri-winchite and ferrowinchite) to sodic (glaucophane and ferroglaucophane), with glaucophane predominating (Table 2 and fig. 1, 2 and 3). The minor green amphiboles forming between the pyroxene and blue amphiboles are actinolite (Table 2, fig. 3).

Muscovite compositions, especially phengite ($K(Al,Mg,Fe)_2Si_4O_{10}(OH)_2$) components, are known to be both temperature and pressure dependant in metamorphic rocks (e.g. Råheim, 1977). An empirical phengite geothermometer/geobarometer has been devised on this basis (Massone and Schreyer, 1987). This amphibolite lacks the equilibrium assemblage for accurate geobarometry (phengite with associated quartz, K-feldspar and phlogopite), but the presence of a ferromagnesian phase (amphibole) indicates that the mica compositions can still be used to give minimum pressures for this assemblage (Massone and Schreyer, 1987). Applying this phengite geobarometer to the amphibolites in this study gives a minimum pressure of around 1000–1200 MPa at the 400–500°C estimated above (fig. 3).

The following reaction has been used as a geobarometer for sodic-amphibole bearing assemblages (Brown, 1977): Ca-amphibole + chlorite + albite + iron oxide $\rightarrow$ Na-amphibole + epidote + water. The present assemblage in these rocks includes epidote and albite but no chlorite or iron oxides are present, so the assemblage has surpassed this equilibrium, and consequently this geobarometer can only give a minimum pressure estimate. Minimum pressures of greater than 700 MPa are thus indicated by this method (fig. 3).

Conclusions

The precursor of this medium-grained, equigranular blue schist/amphibolite was apparently an undeformed dolerite that was initially incipiently metamorphosed under greenschist facies conditions. The amphibolite subsequently underwent high pressure metamorphism under static conditions. The textural evidence indicates a prograde metamorphic path under high pressure but with very little heating, and no shearing. The lack of total mineral equilibration indicates very rapid compression and decompression or exhumation.

The greenschist metamorphism was at about 300 MPa and 350–450°C, while minimum peak metamorphic conditions for phengite and blue amphibole were about 400–500°C and 1000–1400 MPa, which correspond to a depth of burial of the order of 30 km in a low geothermal gradient.

The petrology and the mineral compositions indicate that the assemblage formed by burial to ~30 km in a subducted wedge, with rapid exhumation. This P-T interpretation is consistent with the thrust model of Reed *et al*. (in prep.).

References

BROWN, A. V.; MCCLENAGHAN, M. P.; TURNER, N. J.; BAILLIE, P. W.; MCCLENAGHAN, J.; CALVER, C. R. 1989. Geological atlas 1:50 000 series. Sheet 73 (8112N). Huntley. *Explanatory Report Geological Survey Tasmania*.

BROWN, E. H. 1977. The crossite content of Ca-amphibole as a guide to pressure of metamorphism. *Journal of Petrology* 18:53–72.

DOBRETSOV, N. L. 1975. The glaucophane schist facies. *in:* DOBRETSOV, N. L.; SOBOLEV, V. S.; SOBOLEV, N. V.; KHLESTOV, V. V. (ed.). *The facies of regional metamorphism at high pressures*. 84–153. [Translated by D. A. Brown, ANU, Canberra].

EL-SHAZLY, A. K. 1994. Petrology of lawsonite-, pumpellyite- and sodic amphibole-bearing metabasites from north-east Oman. *Journal Metamorphic Petrology* 12:23–48.

EL-SHAZLY, A. K.; LIOU, J. G. 1991. Glaucophane chloritoid-bearing assemblages from NE Oman: petrologic significance and a petrogenetic grid for high P metapelites. *Contributions to Mineralogy and Petrology* 107:180–201.

ERNST, W. G. 1979. Coexisting sodic and calcic amphiboles from high-pressure metamorphic belts and the stability of barroisitic amphibole. *Mineralogical Magazine* 43:269–278.

EVERARD, J. L. *In prep*. A blue amphibole locality from the northern Arthur Lineament. *Record Tasmanian Geological Survey* 1999/5.

GREEN, T. H.; SPILLER, A. R. 1977. Blue amphibole from Precambrian metabasalts, Savage River, Tasmania. *American Mineralogist* 62:164–166.

IBARGUCHI, J. I. G.; DALLMEYER, R. D. 1991. Hercynian blueschist metamorphism in northern Portugal — tectonothermal implications. *Journal Metamorphic Geology* 9:539–549.

LEAKE, B. E.; WOOLLEY, A. R. ; ARPS, C. E. S.; BIRCH, W. D.; *and others*. 1997. Nomenclature of amphiboles: Report of the Subcommittee on Amphiboles of the International Mineralogical Association Commission on New Minerals and Mineral Names. *Mineralogical Magazine* 405:295–321.

LIOU, J. G.; MARUYAMA, S.; *et al.* 1987. Very low grade metamorphism of volcanic and volcaniclastic rocks — mineral assemblages and mineral facies, *in:* FREY, M. (ed.). *Low temperature metamorphism*. 59–113. Blackie : Glasgow.

MARUYAMA, S.; CHO, M.; LIOU, J. G. 1986. Experimental investigations of blueschist-greenschist transition equilibria: pressure dependence of Al_2O_3 contents in sodic amphiboles — a new geobarometer. *Memoir Paper Geological Society of America* 164:1–16.

MASSONE, H-J.; SCHREYER, W. 1987. Phengite geobarometry based on the limiting assemblage with K-feldspar, phlogopite and quartz. *Contributions Mineralogy and Petrology* 96:212–224.

RÅHEIM, A. 1977. Petrology of the Strathgordon area, western Tasmania: Si^{4+}-content of phengite mica as a monitor of metamorphic grade. *Journal Geological Society of Australia* 24:329–338.

REED, A. R.; CALVER, C. R. BOTTRILL, R. S. (in prep.). A Palaeozoic convergent margin in the West Tamar Region, northern Tasmania: implications for understanding the tectonic evolution of Tasmania and SE Australia.

SCHUMACHER, J. C. 1991. Empirical ferric iron corrections: necessity, assumptions and effects on selected geobarometers. *Mineralogical Magazine* 378:3–18.

SCHUMACHER, J. C. 1997. The estimation of ferric iron in electron microprobe analyses. Appendix 2 *in:* LEAKE, B. E.; WOOLLEY, A. R. ; ARPS, C. E. S.; BIRCH, W. D.; *and others*. Nomenclature of amphiboles: Report of the Subcommittee on Amphiboles of the International Mineralogical Association Commission on New Minerals and Mineral Names. *Mineralogical Magazine* 405:312–321.

SPRY, A. H. 1964. Precambrian rocks of Tasmania, Part VI, the Zeehan–Corinna area. *Papers Proceedings Royal Society of Tasmania* 98:23–48.

TURNER, N. J.; BOTTRILL, R. S. 1993. Blue amphibole in the Proterozoic to Cambrian Arthur Metamorphic Complex, northwest Tasmania. *Report Mineral Resources Tasmania* 1993/26.

TURNER, N. J.; BOTTRILL, R. S. 2001. Blue amphibole, Arthur Metamorphic Complex: Composition and regional tectonic setting. *Australian Journal of Earth Sciences* 48:167–181.

[12 December 2001]

Table 1

Microprobe analyses and structural formulae of micas coexisting with blue amphiboles

No.	*#1*	*#2*	*#3*	*#4*	*#5*	*#6*
SiO_2	49.57	49.26	50.57	48.51	50.52	50.95
TiO_2	0.04	0.13	0.04	0.06	0.08	0.07
Al_2O_3	19.39	19.77	19.38	21.33	19.93	22.36
Cr_2O_3	0.00	0.02	0.03	0.00	0.04	na
V_2O_3	0.02	0.11	0.09	0.04	0.04	na
FeO(t)	8.87	8.92	8.52	8.44	8.49	6.83
MnO	0.00	0.08	0.04	0.05	0.06	0.06
MgO	5.91	5.58	5.59	4.34	5.15	4.11
ZnO	0.00	0.00	0.00	0.00	0.05	na
CaO	0.00	0.00	0.00	0.02	0.00	0.00
Na_2O	0.01	0.03	0.03	0.07	0.02	0.07
K_2O	11.01	10.26	10.85	10.44	10.97	10.92
BaO	0.04	0.00	0.02	0.01	0.04	na
NiO	0.00	0.02	0.00	0.06	0.00	na
F	0.13	0.06	0.09	0.06	0.15	na
Cl	0.07	0.03	0.03	0.01	0.04	na
O=F	0.05	0.03	0.04	0.02	0.06	na
O=Cl	0.01	0.01	0.01	0.00	0.01	na
Total	**95.12**	**94.31**	**95.33**	**93.46**	**95.65**	**95.37**
Si	6.956	6.937	7.039	6.875	7.017	6.852
$Al^{(iv)}$	1.044	1.063	0.961	1.125	0.983	1.148
sum T	*8.000*	*8.000*	*8.000*	*8.000*	*8.000*	*8.000*
$Al^{(vi)}$	2.163	2.217	2.218	2.438	2.280	2.394
Ti	0.004	0.014	0.004	0.007	0.008	0.007
Cr	0.000	0.002	0.003	0.000	0.005	0.000
Fe	1.040	1.050	0.992	1.000	0.986	0.768
V	0.003	0.012	0.011	0.005	0.004	0.000
Zn	0.000	0.000	0.000	0.000	0.005	na
Mn	0.000	0.009	0.005	0.006	0.007	0.007
Mg	1.236	1.170	1.160	0.916	1.067	0.824
sum b	*4.446*	*4.474*	*4.393*	*4.372*	*4.362*	*4.000*
Ca	0.000	0.000	0.000	0.002	0.000	0.000
Ba	0.002	0.000	0.001	0.001	0.002	0.000
Na	0.004	0.008	0.008	0.019	0.007	0.018
K	1.970	1.843	1.927	1.888	1.943	1.873
sum a	*1.976*	*1.851*	*1.936*	*1.910*	*1.952*	*1.892*
F	0.057	0.029	0.039	0.025	0.067	na
Cl	0.016	0.007	0.008	0.002	0.008	na
Cat. Total	*14.422*	*14.325*	*14.329*	*14.282*	*14.314*	*13.892*
T°C\P (Mpa)						
400	1178	1153	1289	1069	1260	1038
500	1298	1273	1409	1189	1380	1158

Table 3

Microprobe analyses and structural formulae of the primary pyroxenes

Anal. No. *Phase*	*#19* *7830B* *px2*	*#20* *7830B* *px3*	*#33* *7830A* *px1*	*#34* *7830A* *px2*
SiO_2	52.88	52.91	50.56	51.21
TiO_2	0.09	0.04	0.40	0.31
Al_2O_3	2.21	0.97	2.20	2.85
Cr_2O_3	0.04	0.04	0.01	0.00
FeO(t)	17.88	18.38	19.80	19.78
MnO	0.22	0.45	0.24	0.32
MgO	7.55	7.30	6.32	5.58
CaO	11.67	13.72	10.20	10.22
Na_2O	5.61	5.10	5.09	6.26
K_2O	0.05	0.01	0.07	0.10
Sum Ox%	**98.20**	**100.00**	**95.70**	**97.84**
final formula, to 6 cations				
Si	2.006	2.009	2.012	1.986
$Al^{(iv)}$	0.000	0.000	0.000	0.014
sum T	*2.006*	*2.009*	*2.012*	*2.000*
$Al^{(vi)}$	0.099	0.043	0.103	0.116
Ti	0.003	0.001	0.012	0.009
Fe'''	0.297	0.311	0.245	0.356
Cr	0.001	0.001	0.000	0.000
Mg	0.427	0.413	0.375	0.322
Fe''	0.173	0.230	0.264	0.197
Mn	0.000	0.000	0.000	0.000
sum b	*1.000*	*1.000*	*1.000*	*1.000*
Mg	0.000	0.000	0.000	0.000
Fe''	0.097	0.042	0.149	0.089
Mn	0.007	0.014	0.008	0.011
Ca	0.474	0.558	0.435	0.425
Na	0.413	0.375	0.393	0.471
K	0.002	0.000	0.004	0.005
sum a	*0.994*	*0.991*	*0.988*	*1.000*
Total	**4.000**	**4.000**	**4.000**	**4.000**
$Mg/Mg+Fe''$	0.711	0.642	0.586	0.621
$Fe'''/Fe'''+Al^{(iv)}$	0.750	0.878	0.704	0.754
100Na/Na+Ca	46.521	40.215	47.452	52.571
Na (B)	0.413	0.375	0.393	0.471
Ca/(Ca+Mg+Fe)	0.4050	0.4488	0.3555	0.411
Classification				
jd	6.7	2.8	7.3	8.2
aeg	20.2	20.0	17.2	25.1
en	29.0	26.6	26.3	22.8
fs	11.8	14.8	18.6	13.9
wo	32.3	35.9	30.6	30.0

Table 2

Microprobe analyses and structural formulae of the amphiboles

Anal. No.	*#31*	*#32*	*#35*	*#38*	*#39*	*#41*	*#45*	*#46*	*#8*	*#13*	*#44*
Phase	*7830A*	*7830A*	*7830A*	*7830A*	*7830A*	*7830A*	*7830A*	*7830A*	*7830B*	*7830B*	*7830A*
	am3	*am4*	*am5*	*am6*	*am7*	*am8*	*am12*	*am13*	*am19*	*am24*	*am11*
SiO_2	53.72	54.50	54.28	55.85	54.52	54.54	55.10	55.32	54.28	55.12	54.53
TiO_2	0.19	0.10	0.07	0.08	0.06	0.07	0.02	0.00	0.03	0.04	0.09
Al_2O_3	4.52	5.17	6.15	6.14	6.85	6.12	6.12	6.55	5.08	6.41	3.67
Cr_2O_3	0.00	0.00	0.01	0.00	0.00	0.00	0.00	0.03	0.00	0.00	0.00
FeO(t)	21.53	20.08	20.31	20.36	20.26	20.80	19.98	20.52	22.50	20.18	20.40
MnO	0.22	0.30	0.22	0.21	0.20	0.18	0.13	0.12	0.18	0.17	0.23
MgO	7.93	8.20	7.13	7.65	7.05	7.76	7.73	6.65	7.04	7.89	9.14
CaO	2.09	1.39	0.74	1.05	1.39	1.70	1.17	1.00	1.49	0.96	2.75
Na_2O	5.83	6.14	6.20	6.35	6.14	5.90	6.19	6.53	6.05	6.34	5.30
K_2O	0.09	0.03	0.02	0.06	0.06	0.16	0.04	0.04	0.04	0.03	0.20
BaO	0.12	0.00	0.00	0.01	0.03	0.00	0.00	0.03	0.02	0.00	0.00
ZrO_2	0.09	0.00	0.01	0.00	0.08	0.02	0.02	0.00	0.02	0.00	0.05
F	0.09	0.09	0.08	0.00	0.10	0.11	0.08	0.06	0.10	0.08	0.10
Cl	0.07	0.00	0.01	0.00	0.02	0.02	0.02	0.03	0.00	0.00	0.02
H_2O(c)	2.00	2.03	2.02	2.12	2.03	2.04	2.05	2.05	2.02	2.07	2.02
O=F	0.04	0.04	0.03	0.00	0.04	0.05	0.03	0.02	0.04	0.03	0.04
O=Cl	0.01	0.00	0.00	0.00	0.00	0.00	0.01	0.01	0.00	0.00	0.00
Sum Ox%	**99.53**	**99.09**	**98.26**	**100.86**	**99.62**	**100.45**	**99.61**	**99.64**	**99.93**	**100.39**	**99.55**
final formula, minimum constraints											
Si	7.922	7.956	7.983	7.982	7.945	7.926	7.977	7.991	7.949	7.944	7.970
$Al^{(iv)}$	0.078	0.044	0.017	0.018	0.055	0.074	0.023	0.009	0.051	0.056	0.030
sum T	*8.000*	*8.000*	*8.000*	*8.000*	*8.000*	*8.000*	*8.000*	*8.000*	*8.000*	*8.000*	*8.000*
$Al^{(vi)}$	0.707	0.845	1.049	1.016	1.121	0.974	1.020	1.105	0.826	1.033	0.602
Ti	0.021	0.011	0.008	0.009	0.007	0.008	0.002	0.000	0.003	0.004	0.010
Fe'''	0.679	0.742	0.652	0.666	0.435	0.436	0.640	0.687	0.736	0.569	0.759
Cr	0.000	0.000	0.001	0.000	0.000	0.000	0.000	0.003	0.000	0.000	0.000
Mg	1.743	1.784	1.563	1.629	1.531	1.681	1.668	1.432	1.537	1.695	1.991
Fe''	1.850	1.618	1.727	1.680	1.906	1.902	1.669	1.773	1.898	1.699	1.639
Mn	0.000	0.000	0.000	0.000	0.000	0.000	0.000	0.000	0.000	0.000	0.000
sum C	*5.000*	*5.000*	*5.000*	*5.000*	*5.000*	*5.000*	*5.000*	*5.000*	*5.000*	*5.000*	*5.000*
Mg	0.000	0.000	0.000	0.000	0.000	0.000	0.000	0.000	0.000	0.000	0.000
Fe''	0.125	0.092	0.119	0.088	0.128	0.191	0.109	0.019	0.122	0.165	0.096
Mn	0.027	0.037	0.027	0.025	0.025	0.022	0.016	0.015	0.022	0.021	0.028
Ca	0.330	0.217	0.117	0.161	0.217	0.265	0.181	0.155	0.234	0.148	0.431
Na	1.517	1.654	1.737	1.726	1.630	1.522	1.693	1.811	1.622	1.666	1.445
sum B	*2.000*	*2.000*	*2.000*	*2.000*	*2.000*	*2.000*	*2.000*	*2.000*	*2.000*	*2.000*	*2.000*
Na	0.150	0.084	0.031	0.034	0.105	0.141	0.044	0.018	0.096	0.106	0.057
K	0.017	0.006	0.004	0.011	0.011	0.030	0.007	0.007	0.007	0.006	0.037
sum A	*0.167*	*0.090*	*0.035*	*0.044*	*0.116*	*0.170*	*0.051*	*0.025*	*0.103*	*0.111*	*0.095*
F	0.042	0.042	0.037	0.000	0.046	0.051	0.037	0.027	0.009	0.000	0.046
Cl	0.017										
Total	**15.167**	**15.090**	**15.035**	**15.044**	**15.116**	**15.170**	**15.051**	**15.025**	**15.103**	**15.111**	**15.095**
total Al	0.785	0.889	1.066	1.034	1.176	1.048	1.044	1.115	0.877	1.089	0.632
total Fe	2.655	2.452	2.499	2.433	2.469	2.529	2.419	2.479	2.756	2.433	2.494
Mg/Mg+Fe''	0.485	0.524	0.475	0.492	0.445	0.469	0.500	0.447	0.447	0.499	0.549
Fe'''/Fe'''+$Al^{(iv)}$	0.490	0.467	0.383	0.396	0.280	0.309	0.386	0.383	0.471	0.355	0.558
100Na/Na+Ca	82.122	88.382	93.707	91.479	88.251	85.182	90.320	92.127	87.401	91.829	77.036
100Al/Si+Al	9.020	10.053	11.777	11.468	12.895	11.677	11.572	12.243	9.932	12.051	7.347
Na (B)	1.517	1.654	1.737	1.726	1.630	1.522	1.693	1.811	1.622	1.666	1.445
$Al^{(iv)}$	0.078	0.044	0.017	0.018	0.055	0.074	0.023	0.009	0.051	0.056	0.030
Classification	Fe-Gl	Gl	Fe-Gl	Fe-Gl	Fe-Gl	Fe-Gl	Fe-Gl	Fe-Gl	Fe-Gl	Fe-Gl	Fe3W

Table 2 (continued)

Anal. Number	#4	#9	#5	#29	#10	#11	#12	#6	#7
Phase	*7830B am15*	*7830B am20*	*7830B am16*	*7830A am1*	*7830B am21*	*7830B am22*	*7830B am23*	*7830B am17-gn*	*7830B am18-gn*
SiO_2	54.58	52.81	54.07	51.44	52.79	52.23	54.00	54.16	54.50
TiO_2	0.10	0.00	0.00	0.55	0.10	0.04	0.06	0.03	0.00
Al_2O_3	3.36	4.23	4.88	4.71	3.95	1.39	3.21	1.27	1.25
Cr_2O_3	0.02	0.00	0.00	0.04	0.00	0.00	0.01	0.06	0.02
FeO(t)	19.98	21.38	23.19	20.48	21.76	30.50	23.78	14.78	14.77
MnO	0.21	0.27	0.17	0.24	0.21	0.49	0.25	0.36	0.38
MgO	9.64	9.26	7.16	7.82	8.84	4.18	7.69	14.41	14.64
CaO	3.26	4.67	2.33	3.01	4.73	4.11	2.94	11.44	11.41
Na_2O	4.88	4.02	5.56	5.41	4.05	4.09	5.13	0.81	0.84
K_2O	0.08	0.05	0.05	0.12	0.11	0.11	0.10	0.10	0.07
BaO	0.00	0.00	0.04	0.04	0.05	0.05	0.00	0.00	0.00
ZrO_2	0.10	0.10	0.03	0.05	0.28	0.00	0.00	0.05	0.00
F	0.07	0.06	0.09	0.12	0.01	0.06	0.06	0.06	0.10
Cl	0.01	0.00	0.02	0.08	0.02	0.31	0.11	0.01	0.01
H_2O(c)	2.04	2.04	2.03	1.92	2.05	1.88	2.00	2.04	2.04
O=F	0.03	0.03	0.04	0.05	0.01	0.02	0.03	0.02	0.04
O=Cl	0.00	0.00	0.00	0.02	0.00	0.07	0.02	0.00	0.00
Sum Ox%	99.42	100.13	100.73	96.84	100.06	100.57	100.52	99.83	100.34
final formula, minimum constraints									
Si	7.980	7.809	7.925	7.823	7.841	7.982	7.952	7.861	7.864
$Al^{(iv)}$	0.020	0.191	0.075	0.177	0.159	0.018	0.048	0.139	0.136
sum T	*8.000*	*8.000*	*8.000*	*8.000*	*8.000*	*8.000*	*8.000*	*8.000*	*8.000*
$Al^{(vi)}$	0.559	0.546	0.768	0.667	0.532	0.232	0.508	0.078	0.076
Ti	0.011	0.000	0.000	0.063	0.011	0.005	0.007	0.003	0.000
Fe'''	0.731	0.473	0.592	0.495	0.450	0.899	0.787	0.154	0.169
Cr	0.002	0.000	0.000	0.005	0.000	0.000	0.001	0.007	0.002
Mg	2.101	2.041	1.564	1.772	1.957	0.952	1.688	3.117	3.148
Fe''	1.596	1.940	2.075	1.999	2.049	2.913	2.009	1.640	1.604
Mn	0.000	0.000	0.000	0.000	0.000	0.000	0.000	0.000	0.000
sum C	*5.000*	*5.000*	*5.000*	*5.000*	*5.000*	*5.000*	*5.000*	*5.000*	*5.000*
Mg	0.000	0.000	0.000	0.000	0.000	0.000	0.000	0.000	0.000
Fe''	0.117	0.231	0.175	0.112	0.204	0.086	0.132	0.000	0.010
Mn	0.026	0.034	0.021	0.031	0.026	0.063	0.031	0.044	0.046
Ca	0.511	0.740	0.366	0.490	0.753	0.673	0.464	1.779	1.764
Na	1.347	0.995	1.438	1.367	1.017	1.177	1.373	0.177	0.180
sum B	*2.000*	*2.000*	*2.000*	*2.000*	*2.000*	*2.000*	*2.000*	*2.000*	*2.000*
Na	0.037	0.157	0.142	0.229	0.150	0.035	0.092	0.051	0.055
K	0.015	0.009	0.009	0.023	0.021	0.021	0.019	0.019	0.013
sum A	*0.052*	*0.167*	*0.152*	*0.252*	*0.171*	*0.056*	*0.111*	*0.070*	*0.068*
F	0.046	0.047	0.014	0.058	0.132	0.000	0.000	0.023	0.000
Cl									
Total	**15.052**	**15.167**	**15.152**	**15.252**	**15.171**	**15.056**	**15.111**	**15.070**	**15.068**
total Al	0.579	0.737	0.843	0.844	0.691	0.250	0.557	0.217	0.213
total Fe	2.443	2.644	2.843	2.605	2.704	3.898	2.928	1.794	1.783
$Mg/Mg+Fe''$	0.568	0.513	0.430	0.470	0.488	0.246	0.457	0.655	0.662
$Fe'''/Fe'''+Al^{(iv)}$	0.566	0.464	0.435	0.426	0.458	0.795	0.608	0.664	0.688
100Na/Na+Ca	72.503	57.356	79.711	73.589	57.457	63.628	74.742	9.041	9.241
100Al/Si+Al	6.763	8.624	9.612	9.738	8.102	3.040	6.546	2.689	2.631
Na (B)	1.347	0.995	1.438	1.367	1.017	1.177	1.373	0.177	0.180
$Al^{(iv)}$	0.020	0.191	0.075	0.177	0.159	0.018	0.048	0.139	0.136
Classification	Fe3W	W	Fe2W	Fe2W	Fe2W	Fe23W	Fe23W	Act	Act

Table 4

Microprobe analyses of albite, epidote and sphene

Anal. No.	*#2*	*#37*	*#20*
Phase	*7830B-ab2 albite*	*7830A-pl1 albite*	*7830B-sphene sphene*
SiO_2	68.18	68.76	28.35
TiO_2	0.00	0.01	39.73
Al_2O_3	20.16	19.92	1.95
FeO(t)	0.16	0.09	2.64
Mn_2O_3	0.00	0.02	
MnO			0.13
MgO	0.00	0.00	0.01
CaO	0.26	0.09	26.46
SrO	0.00	0.00	
BaO	0.12	0.07	
Na_2O	11.33	10.89	0.03
K_2O	0.07	0.18	0.09
Rb_2O	-	-	
P_2O_5	0.00	0.00	
Sum Ox%	**100.28**	**100.03**	**99.39**
final formula	*8 cations*	*8 cations*	*5 oxygens*
Si	2.973	2.996	0.931
$Al^{(iv)}$	0.027	0.004	0.076
sum T	*3.000*	*3.000*	*1.007*
$Al^{(vi)}$	1.009	1.018	
Ti	0.000	0.000	0.981
Fe'''	0.006	0.003	0.073
Cr	0.000	0.000	0.000
Mg	0.000	0.000	0.001
Mn	0.000	0.000	0.003
sum b	*1.015*	*1.022*	*1.058*
Ca	0.012	0.004	0.931
Sr	0.000	0.000	
Ba	0.002	0.001	
Na	0.958	0.920	0.002
K	0.004	0.010	0.004
sum a	*0.976*	*0.935*	*0.937*
Total	**4.990**	**4.958**	**3.000**
Classification			
ab	98.2	98.4	
an	1.2	0.4	
or	0.4	1.1	
cs	0.2	0.1	

Anal. No.	*#1*	*#17*	*#40*
Phase	*7830B-ep2 epidote*	*7830B-ep3 epidote*	*7830A-ep1 epidote*
SiO_2	37.43	36.99	36.55
TiO_2	0.03	0.07	0.11
Al_2O_3	21.50	20.97	20.79
Cr_2O_3	0.00	0.06	0.02
FeO(t)	14.84	15.28	14.77
Mn_2O_3	0.09	0.01	0.15
MgO	0.04	0.02	0.19
CaO	22.98	23.31	22.15
La_2O_3	0.00	0.00	0.09
Ce_2O_3	0.01	0.00	0.01
Y_2O_3	0.06	0.00	0.00
H_2O(c)	1.86	1.86	1.83
Sum Ox%	**98.84**	**98.57**	**96.66**
final formula, to 8 cations			
Si	2.996	2.971	2.989
$Al^{(iv)}$	0.004	0.029	0.011
sum T	*3.000*	*3.000*	*3.000*
$Al^{(vi)}$	2.023	1.956	1.993
Ti	0.002	0.004	0.007
Fe'''	0.979	1.026	1.011
Cr	0.000	0.004	0.001
Fe''	0.000	0.000	0.000
Mg	0.000	0.002	0.000
Mn	0.000	0.001	0.000
sum b	*3.004*	*2.994*	*3.011*
Mn	0.005	0.000	0.009
Fe	0.014	0.000	0.000
Mg	0.005	0.000	0.023
Ca	1.971	2.006	1.941
Na	0.000	0.000	0.014
K	0.001	0.000	0.001
sum a	*1.996*	*2.006*	*1.989*
Total	**8.000**	**8.000**	**8.000**
%Ps	32.603	34.416	33.651

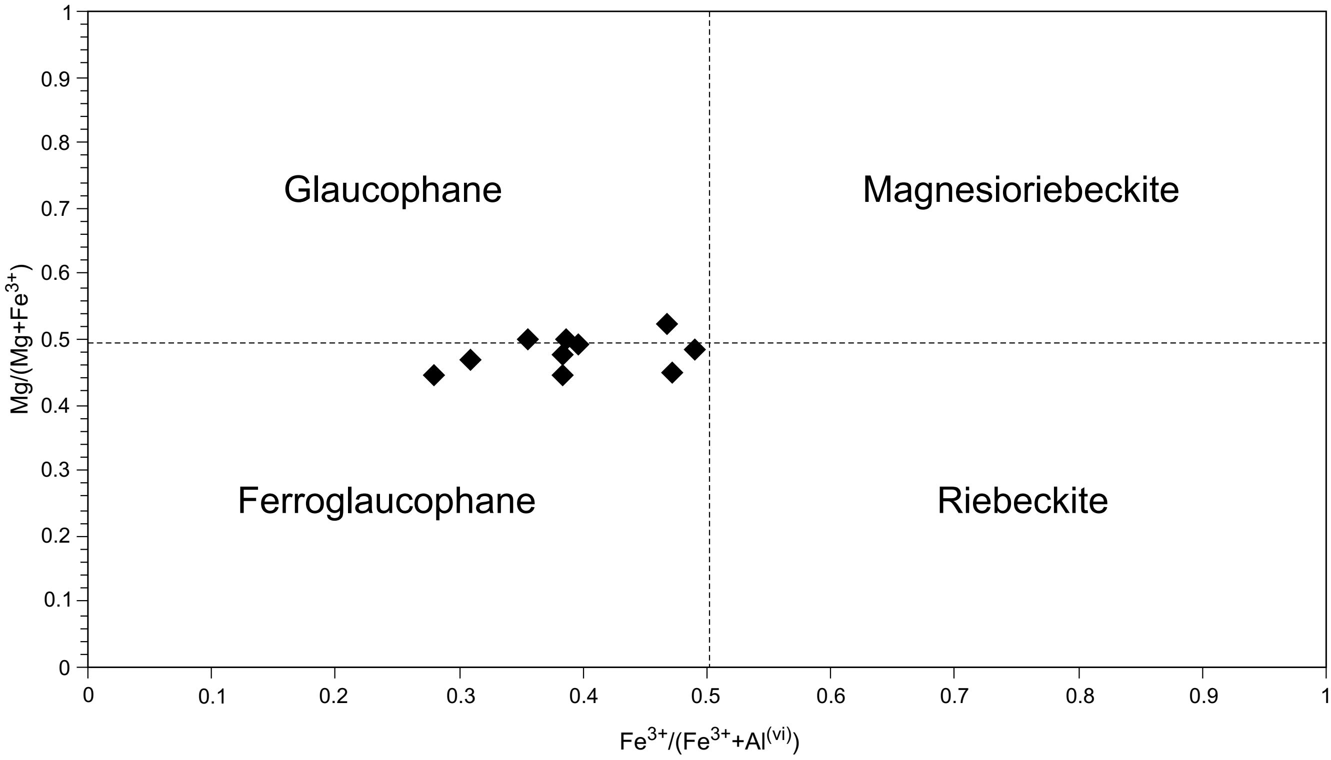

Figure 1

Sodic amphiboles (with NaB >1.5): Mg/(Mg+Fe^{2+}) vs Fe^{3+}/(Fe^{3+}+Al^{vi}), with compositional fields from Leake et al. (1997).

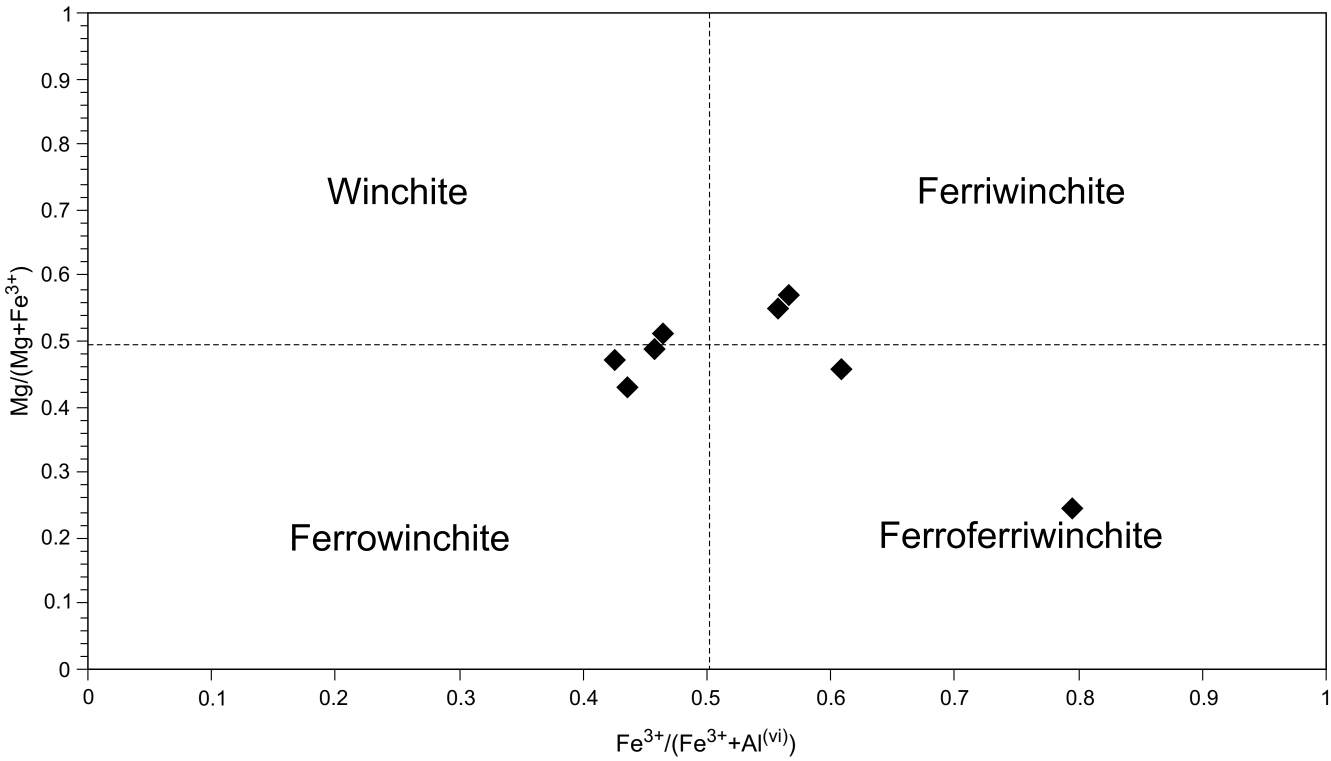

Figure 2

Sodic-calcic amphiboles (with 0.5 > NaB >1.5): Mg/(Mg+Fe^{2+}) vs Fe^{3+}/(Fe^{3+}+Al^{vi}), with compositional fields from Leake et al. (1997).

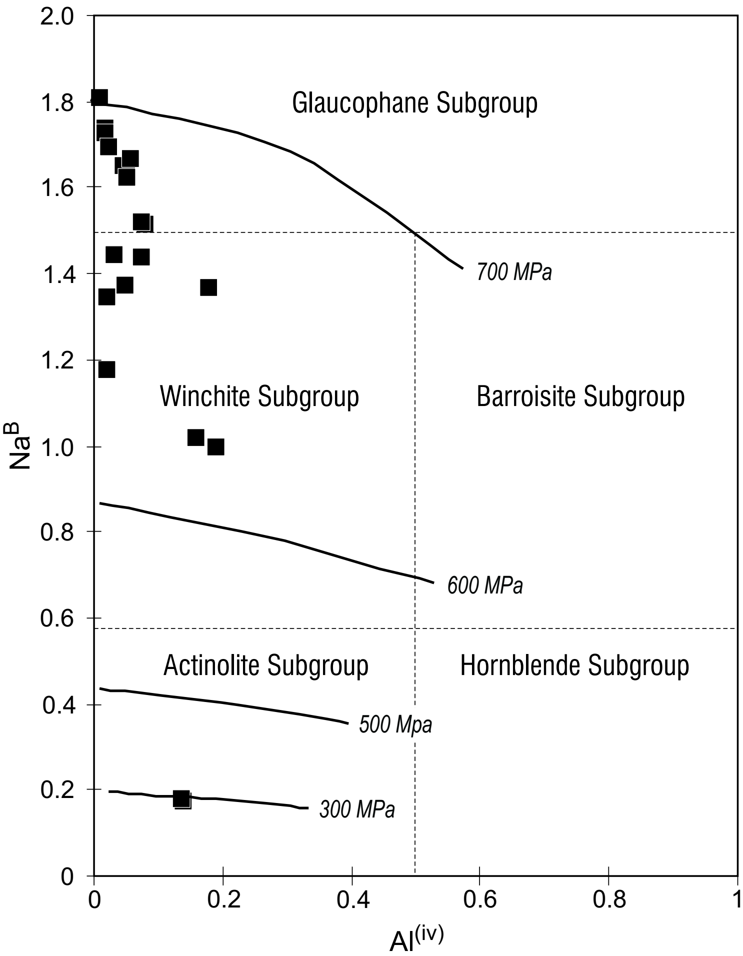

Figure 3

Amphiboles: NaB vs Al iv, with compositional fields from Leake et al. (1997). Isobars shown from

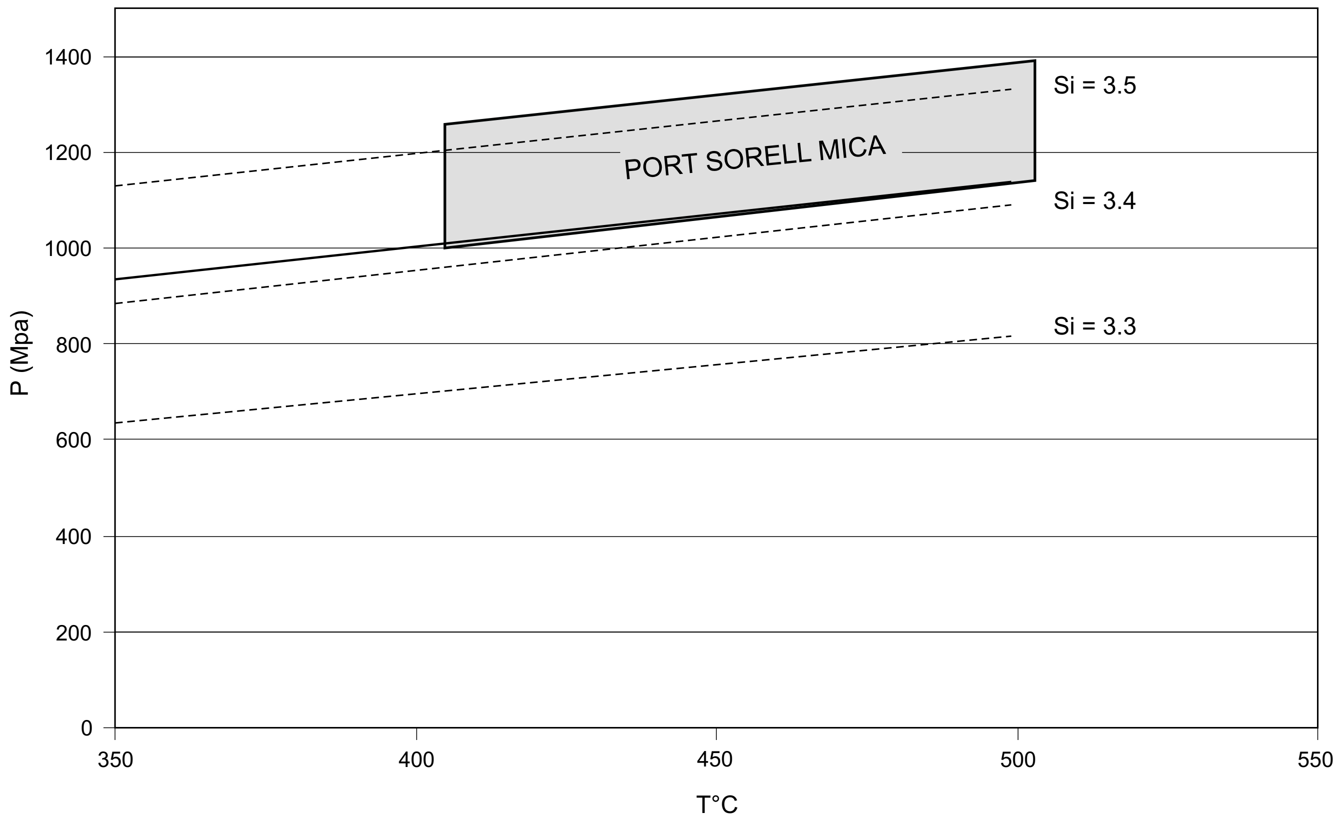

Figure 4

Micas: the graphical relationship of the relationship between the phengite content (expressed as Si atoms/10 (O,OH,F) and temperature and pressure.

Table 5

Mineral reactions shown on Figure 5

Reaction No.	*Reaction*	*Reference*
1	Act + Ab + Mt → Ep + Crossite	Ibarguchi and Dallmeyer, 1991
2	Mg-Chl + Ab + w → Pg + Mg-Gl + Q	El-Shazly and Liou, 1991
3	Fe-Chl + Ab + w → Pg + Fe-Gl + Q	El-Shazly and Liou, 1991
4	Cz + Chl + Tr + Q → Hbd + w	Liou *et al.*, 1987
5	Pm + Chl + Q → Cz + Tr + w	Liou *et al.*, 1987
6	Lw + Pm → Cz + Chl + Q + w	Liou *et al.*, 1987
7	Lw + Gl → Ab + Pm + Chl + Q + w	Liou *et al.*, 1987
8	Lw + Pm + Ab → Cz + Gl + Q + w	Liou *et al.*, 1987
9	Lw + Gl → Ab + Cz + Chl + Q + w	Liou *et al.*, 1987
10	Pm + Chl + Ab → Cz + Gl + w	Liou *et al.*, 1987
11	Pm + Gl + Q → Cz + Tr + Ab + w	Liou *et al.*, 1987
12	Tr + chl + Ab → Gl + Cz + Q + w	Maruyama *et al.*, 1986
13	Tr + chl + Ab → Pm + Gl + Q + w	Liou *et al.*, 1987
14	Ab → Jd + Q	El-Shazly, 1994
15	Chl + Ctd + Q → Alm + w	Dobretsov, 1975

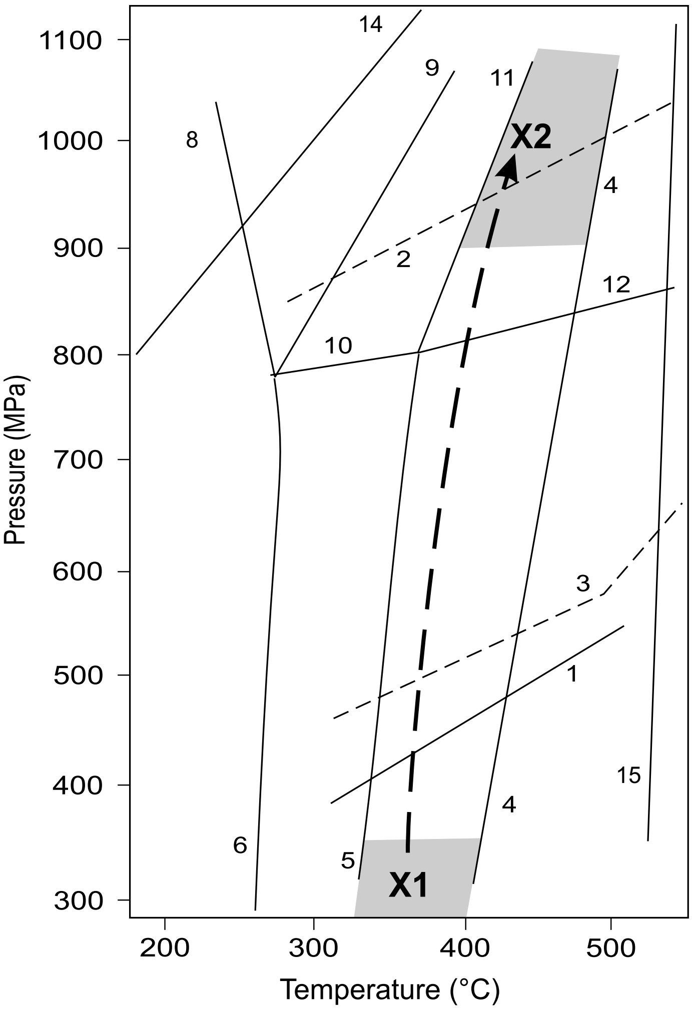

Figure 5

P-T diagram, showing a petrogenetic grid for NCFMASH using published data for metamorphosed basic assemblages. See Table 5 for reactions and abbreviations. The early and peak metamorphic conditions determined here are represented by X1 and X2 respectively. A prograde path that is consistent with the observed minerals is shown.

Abbreviations

Act	actinolite
Ab	albite
Alm	almandine
Chl	chlorite
Ctd	chloritoid
Cz	clinozoisite
Ep	epidote
Gl	glaucophane
Hbd	hornblende
Jd	jadeite
Lw	lawsonite
Mt	magnetite
Pg	paragonite
Pm	pumpellyite
Q	quartz
Tr	tremolite
w	water